INSTITUTE OF PHYSICS PUBLISHING PHYSIOLOGICAL MEASUREMENT

Physiol. Meas. **22** (2001) 693–711 PII: S0967-3334(01)24107-0

A method to standardize a reference of scalp EEG recordings to a point at infinity

Dezhong Yao

Key Laboratory of Biomedical Signal Detection and Intelligent Signal Processing, Department of Automation, University of Electronic Science and Technology of China, Chengdu 610054, People's Republic of China

E-mail: dyao@uestc.edu.cn

Received 19 April 2001
Published 1 October 2001
Online at stacks.iop.org/PM/22/693

Abstract

The effect of an active reference in EEG recording is one of the oldest technical problems in EEG practice. In this paper, a method is proposed to approximately standardize the reference of scalp EEG recordings to a point at infinity. This method is based on the fact that the use of scalp potentials to determine the neural electrical activities or their equivalent sources does not depend on the reference, so we may approximately reconstruct the equivalent sources from scalp EEG recordings with a scalp point or average reference. Then the potentials referenced at infinity are approximately reconstructed from the equivalent sources. As a point at infinity is far from all the possible neural sources, this method may be considered as a reference electrode standardization technique (REST). The simulation studies performed with assumed neural sources included effects of electrode number, volume conductor model and noise on the performance of REST, and the significance of REST in EEG temporal analysis. The results showed that REST is potentially very effective for the most important superficial cortical region and the standardization could be especially important in recovering the temporal information of EEG recordings.

Keywords: electro-encephalogram, reference at infinity, average reference, reference electrode, spectral analysis, equivalent source technique, visual evoked potential

1. Introduction

Both the evoked potential (EP) and the spontaneous potential (EEG) of neural activities are currently read in terms of components thought to reflect distinct neural generators (Desmedt *et al* 1990, Niedermeyer and Lopes da Silva 1999). Each component can be defined by characteristics such as polarity, scalp region, spectra, range of latencies and voltages. Moreover, for these

characteristic values, a potential with zero reference is the desired original data. However, it is well known that, in nature, only the difference between two potentials can be measured, so it is indispensable to set a reference in human scalp recordings (Geselowitz 1998). The cephalic electrode, non-cephalic electrode, earlobe reference, neck reference, average reference etc each yields some effects on the recordings, so different reference sites have been recommended for studies of different potentials (Wolpaw and Wood 1982, Desmedt *et al* 1990).

As neural electrical activation is a spatio-temporal process, the effect of an active reference also is in both spatial and temporal aspects. The effect of a reference on spatial aspect can be summarized with the following comments. (1) The reference will not affect the use of noiseless scalp potentials to solve the inverse problem; i.e. the localization of neural active sources will not depend on the reference (Pascual-Marqui *et al* 1993). However, if some noise is added to the scalp recordings, the choice of a reference may affect the signal-to-noise ratio at given electrode sites. Accordingly the 'optimal' reference electrode for electric source imaging depends on the region of interest on the cortex (Gencer *et al* 1996). (2) The effect of the reference choice on the shape of an EEG contour map depends on the number and spacing of the contour lines. A change of the reference will add or subtract a constant value at all locations, like raising or lowering the water level in a landscape, without changing the surface (Geselowitz 1998).

The effect of a reference on temporal aspect is due to the activity at the reference electrode. A body surface point or the average is active means that the actual potential, if referenced at a neutral point, at the point is different for different latencies (Desmedt *et al* 1990, Geselowitz 1998). Apparently, an active reference will affect the temporal dynamic analysis and spectral analysis of the EEG time course because a non-constant temporal component is added to the time course. To solve this problem, a neutral potential is desired to act as the reference, and the potential at infinity is the ideal one since a point at infinity is far from the neural sources, thus bringing no effect on EEG recordings.

In the literature, the neutral reference and zero of potential have been a controversial topic for a long time (Wolpaw and Wood 1982, Desmedt *et al* 1990, Pascual-Marqui *et al* 1993). In this paper, we are not interested in finding a neutral reference or an approximate zero of potential on the scalp because it is an unsolvable problem. There is no point on the scalp surface whose potential can be considered to be zero (Geselowitz 1998).

In this work, a method, termed REST (reference electrode standardization technique), is proposed to approximately transform a scalp point or the average reference to a reference point at infinity. The transformation is based on the bridge—the common origin of the two potentials before and after transformation, i.e. the actual neural sources or their equivalent sources (Yao 1995a, 1996, 2000a, Yao *et al* 2001). The algorithm is shown in the following section 2 and then is investigated by simulations in sections 3 and 4. In section 5, extensive discussions are given which include the differences and relations among REST, the cortical imaging technique (CIT), the scalp Laplacian mapping technique (LMT) and the magneto-encephalogram (MEG).

2. REST: reference electrode standardization technique

2.1. The scalp EEG recording model

The scalp potentials can be represented as

$$V = GX \tag{1}$$

where the matrix V with size $l \times k$ represents scalp potential recordings at l electrodes with k samples, the matrix X with size $m \times k$ represents k samples of m neural source signals in the

head model, and the matrix G with size $l \times m$ is the transfer function determined by the head model, source model and electrode montage. In general, the derivation of the transfer matrix implicitly assumes that the potential generated by a dipole is zero at infinity (de Munck 1988, Yao 2000b), so the forward potential calculated by equation (1) is a recording with reference at infinity.

In practice, since only the difference between two potentials can be measured, it is necessary to set a physical point as reference on the scalp. Supposing an electrode such as the one near an earlobe is the reference, the potential at this electrode referenced at infinity is

$$\boldsymbol{v}_e = \boldsymbol{g}_e X \tag{2}$$

where the row vector $\boldsymbol{g}_e$ with size $1 \times m$ is formed by the row in G corresponding to the reference electrode, and the row vector $\boldsymbol{v}_e$ with size $1 \times k$ is the row vector in V corresponding to the reference electrode. Based on equations (1) and (2), we have the scalp EEG recording model with a scalp reference

$$V_e = V - \boldsymbol{t}\boldsymbol{v}_e = GX - \boldsymbol{t}\boldsymbol{g}_e X = (G - \boldsymbol{t}\boldsymbol{g}_e)X = G_e X \tag{3}$$

where $\boldsymbol{t}$ is a column vector with size $l \times 1$ and each of its elements being unity. G_e is the transfer matrix. Similarly, we can choose the average of the scalp potentials as the reference. The average over all sensors is

$$\boldsymbol{v}_a = \text{average}(V) = \frac{1}{l}\boldsymbol{t}' V = \frac{1}{l}\boldsymbol{t}' G X \tag{4}$$

where $\boldsymbol{v}_a$ is a row vector with size $1 \times k$, and the operator 'average' means the average of the recordings over all sensors temporally sample by sample. $\boldsymbol{t}'$ is the transpose of $\boldsymbol{t}$. Finally, we have the scalp EEG recording model with the average reference

$$\boldsymbol{V}_a = V - \boldsymbol{t}\boldsymbol{v}_a = GX - \frac{1}{l}\boldsymbol{t}\boldsymbol{t}' G X = \left(G - \frac{1}{l}\boldsymbol{t}\boldsymbol{t}' G\right) X = G_a X. \tag{5}$$

Equations (1), (3) and (5) show the scalp recording models with reference respectively at infinity, a body electrode and the average.

In practice, the potential referenced at the average is obtained not from the potential V, which is unknown, but from the potential V_e, which is the practical recording. It is easy to prove that

$$V_a = V_e - \boldsymbol{t}\,\text{average}(V_e) \tag{6}$$

and

$$V_e = V_a - \boldsymbol{t}\boldsymbol{v}_{ae} \tag{7}$$

where the row vector $\boldsymbol{v}_{ae}$ is formed by the row of the matrix V_a pertaining to the selected reference electrode. Equations (6) and (7) denote that V_a and V_e can be deduced from each other, so they provide the same biophysical information.

2.2. The equivalent source technique

The above three scalp recording models are similar to one another in their mathematical forms. If the inverses of the three transfer matrices exist, each of the three recordings can reconstruct the sources correctly, i.e. the inverse solution will not depend on the reference (Pascual-Marqui *et al* 1993), and then the recordings with reference at infinity can be obtained by a forward calculation of the obtained sources according to equation (1). In mathematics, the maximum number of independent recordings is l in the recording model represented by equation (1), and if $m < l$, equation (1) is an overdetermined problem. For an earlobe reference, one of

the l channels is used as the reference whose potential is usually assumed to be relatively inactive. For the average reference, the assumed average$(V_a) = 0$ denoting that any one of the l channels is a linear combination of the other $l-1$ channels. Apparently, the maximum number of independent channels either with an earlobe reference or the average reference is $l-1$, then only when $m < l-1$ are equations (2) and (3) overdetermined problems. For an overdetermined problem ($m < l-1 < l$), it is possible to solve it by an algorithm, so the neural electric sources could be approximately recovered from any one of the three scalp recordings. However, it is very difficult for an EEG inverse problem to determine simultaneously the number of sources and their locations, strengths and orientations, and there is a theoretical limitation that the solution to the EEG inverse problem is non-unique (Yao 2000a, Yao *et al* 2001).

In this work, our goal is not the EEG inverse but a reference standardization. For this problem, the non-uniqueness of the EEG inverse is not a problem but a way to our goal. In fact, it is the non-uniqueness that provides the theoretical base of the equivalent source technique (EST), which is utilized to approximately recover the scalp potentials with reference at infinity in this work. In recent years, three versions of EST have been developed, where the equivalent sources are a dipole layer (Sidman *et al* 1992), a charge layer (Yao 1995a, 1996), and a multi-pole series at the origin of the coordinate system (Yao 2000a). The three kinds of equivalent source are consistent in theory; the other two can be deduced when one is known (Yao 2000a).

Here the dipole layer was chosen as the equivalent sources of the actual sources for its simplicity in realization and relative better performance (Yao *et al* 2001). In theory, the equivalent dipole or charge layer of actual sources is a continuous and closed layer that encloses all the actual sources inside, and the equivalence means that the layer produces the same potential in the outer region of the layer as that generated by the actual sources (Jackson 1975, Yao 1995b, 2000a, Yao and Luo 1996, Yao *et al* 2001). In practice, for computer implementation, a discrete approximation of the continuous layer was further assumed (Sidman *et al* 1992, Yao 1995a, 1996, He *et al* 1996, Babiloni *et al* 1997, Wang and He 1998, Yao *et al* 2001). As the positions of the discrete equivalent dipole sources were assumed, the inversion of the equivalent sources is a linear problem, which is much easier than the general non-linear search to obtain the actual neural sources in an EEG inverse problem. Besides, in order to have a good approximation of the continuous layer, the number of the equivalent sources is generally much larger than the scalp recording number l, so the problem is an underdetermined problem. The unique minimum norm linear inversion is the general choice for such a problem to obtain the equivalent sources (Sidman *et al* 1992, Yao 1995a), and such an inversion can be easily conducted by a general inverse of the transfer matrix, such as the singular value decomposition (SVD) algorithm.

EST was primarily used in geophysical data processing (Dampney 1969), and recently it was used to obtain the cortical surface potential (CIT) (Sidman *et al* 1992, Yao *et al* 2001). In this work, it was used to obtain the potential with reference at infinity.

2.3. Standardization algorithm

Based on EST, the sources X in equations (1), (3) and (5) may be either the actual sources or their equivalent dipole sources; here they are assumed to be the equivalent dipole sources, then using equations (1) and (5) we obtain

$$V = GX \approx V' = G\left(G_a^+ V_a\right) = \left(GG_a^+\right) V_a = R_a V_a. \tag{8}$$

Here V' is the approximately restored V by using the approximately reconstructed equivalent sources $X \approx G_a^+ V_a$, the matrix R_a is the average reference standardization matrix and the sign

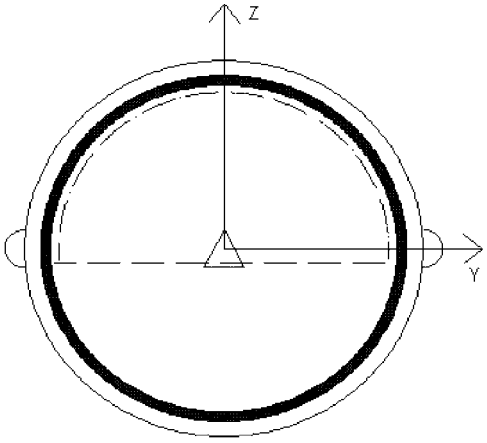

Figure 1. Three-concentric-sphere head volume conductor model. The triangle shows the nose. The centre of the spheres is defined as the coordinate origin. The axis directed away from the origin toward the left ear is defined as the $+y$ axis, and that from the origin to the nasion is the $+x$ axis. The $+z$ axis is defined as the axis that is perpendicular to both these axes and directed from the origin to the vertex. The radii of the three concentric spheres are 0.87 (inner radius of the skull), 0.92 (outer radius of the skull) and 1.0 (radius of the head), while the conductivities are 1.0 (brain and scalp) and 0.0125 (skull). The closed equivalent layer is shown by the dashed line; it is formed by a spherical cap with radius 0.869, and a transverse plane at $z = -0.076$.

'+' denotes the general inverse which is completed by SVD in the following simulation study. For the earlobe reference recordings, we have

$$V = GX \approx V' = G\left(G_e^+ V_e\right) = \left(GG_e^+\right) V_e = R_e V_e \tag{9}$$

where R_e is the earlobe reference standardization matrix.

As $V = V_a + \boldsymbol{t}\,\text{average}(V) = V_a + \boldsymbol{t}\boldsymbol{v}_a$, $V' = V'_a + \boldsymbol{t}\,\text{average}(V') = V'_a + \boldsymbol{t}\boldsymbol{v}'_a$ and we know the V_a, the result of the standardization is further chosen to be

$$V' = V_a + \boldsymbol{t}\boldsymbol{v}'_a. \tag{10}$$

Apparently, the error between V_a and the standardized V'_a is avoided by using equation (10) as the final result, and the remaining error is only the difference between the objective average(V) and the restored average(V').

In equations (8) and (9), R_a and R_e are determined by four factors: the volume conductor model, the equivalent source model, the electrode montage and the calculation of the general inverse, and they are independent of the actual neural sources inside the equivalent source layer, so they can be equally applied to both simulated recordings where the sources are known and empirical recordings where the sources are unknown.

In this work, the usual three-concentric-sphere model was used as the head model (Rush and Driscoll 1969). As shown in figure 1, the radii of the three concentric spheres are 0.87 (inner radius of the skull), 0.92 (outer radius of the skull) and 1.0 (radius of the head), and the conductivities are 1.0 (brain and scalp) and 0.0125 (skull). The forward theory of the three-concentric-sphere model is given by Yao (2000a). A total of $l = 128$ electrodes are uniformly distributed on the upper spherical cap with the lowest latitude being 100 degrees, a little lower than the equator plane of the sphere. While for testing the effects of head model and electrode number, some different head models and electrode montages are used and illustrated in the corresponding sections. For the discrete equivalent dipole layer sources, a closed surface was first formed by a spherical cap surface with radius

$r = 0.869$ and a transverse plane at $z = -0.076$ (dashed lined in figure 1), then a discrete approximation of the continuous layer was further assumed, which included 2600 radial dipoles on the spherical cap surface and 400 radial dipoles on the transverse plane, so the total number of the equivalent sources was $m = 2600 + 400 = 3000$. Due to the limited spherical cap electrode configuration, the theoretically closed dipole layer could not be perfectly reconstructed, the equivalence between the inverted dipole layer and the neural sources inside the layer is approximate and the approximation is different for different dipole locations and orientations (Sidman *et al* 1992, Yao 1995a, 1996, Yao and Luo 1996, He *et al* 1996, Babiloni *et al* 1997, Wang and He 1998, Yao *et al* 2001), so the efficiency of REST will be different for different dipole locations and orientations as shown by the following simulation results.

The general inverses in equations (8) and (9) are alterable with different singular-value truncations, and such a truncation has been used to repress the effect of noise in the scalp recordings on the inverse solution in techniques such as EST (Sidman *et al* 1992, Yao 1996, Yao *et al* 2001). However, while the truncation reduces the effects of measurement noise on the reconstructed cortical potential, it also imposes a severe loss of information because of the exclusion of some high-frequency components (Gencer *et al* 1996). For REST, our purpose is to provide an objective tool to approximately standardize the reference, so any subjective singular value truncation should be avoided. Defining the condition number (CN) as the ratio of the singular value pertaining to the truncation point to the first singular value, for the transfer matrix G_a for the 128-electrode montage and 3000 equivalent dipoles explained above, we found that CN changed smoothly from $\mathrm{CN}(1) = 1.0$ to $\mathrm{CN}(127) = 8.4 \times 10^{-3}$, and then a sharp decrease occurred after 127 with a $\mathrm{CN}(128) = 4.5284 \times 10^{-6}$, so the truncation point was chosen at 127. For G_e, CN changed smoothly from the beginning $\mathrm{CN}(1) = 1.0$ to the end $\mathrm{CN}(127) = 3.9 \times 10^{-3}$, so the total 127 singular values of G_e were kept in the inversion. In fact, as pointed out in section 2.2, the number 127, i.e. $l - 1$, is the maximum number of independent observations in the $l = 128$-electrode montage for both the earlobe reference and the average reference. For other electrode configurations tested below, the truncation point for the related *Ga* also was objectively chosen at the related $l - 1$ for the same reasons.

In summary, REST consists of the following steps.

1. The electrode montage and the scalp recordings V_a are given.
2. A head model such as the three-concentric-sphere model shown in figure 1 is assumed.
3. An equivalent source model such as the discrete dipole layer sources model shown by the dashed line in figure 1 is assumed.
4. Based on the electrode montage, head model and equivalent source model, calculate the transform matrix G in equation (1) and G_a in equation (5) by using the forward theory (Yao 2000a).
5. Calculate the general inverse G_a^+ of the matrix G_a by SVD.
6. Calculate the standardization matrix R_a in equation (8) from the known G and G_a^+.
7. Calculate the $V' = R_a V_a$ as shown by equation (8), and then calculate $\boldsymbol{v}'_a = \mathrm{average}(V')$.
8. Calculate the finial reconstructed EEG recordings V' according to equation (10) by the known recordings V_a and the recovered $\boldsymbol{v}'_a$.

For another reference such as the earlobe reference, the calculation process is similar.

3. Simulation study (I): effectiveness of REST

3.1. Simulation description

The temporal process of a dipolar neural source was simulated by a damped Gaussian function

$$h(t_i) = \exp\left(-\left(2\pi f \frac{t_i - t_0}{\gamma}\right)^2\right)\cos(2\pi f(t_i - t_0) + \alpha) \qquad i = 1, \ldots, k \tag{11}$$

where $t_i = i^* dt$, $k = 256$ and $dt = 0.004$ s $= 4$ ms. We chose this function just because it looks like an evoked potential; the standardization algorithm is independent of any choice of the temporal process. The values of the parameters t_0, f, γ and α are shown in the following sections for each concrete source. Using the function h and the above forward model equations (1), (3) and (5), we derived the spatio-temporal recordings V, V_e and V_a with size $l \times k$.

The relative error (RE) is used to evaluate the effectiveness of REST, and it is

$$\mathrm{RE} = \|V - V_*\| \big/ \|V\| \tag{12}$$

where V is the forward spatio-temporal recording with reference at infinity, and V_* is an alternative of the recording V_e, V_a as well as the restored V, i.e. the V' in equations (8)–(10). The matrix norm $\|*\|$ is defined as $\|V\| = \left(\sum_i \sum_{j=1}^{k} v_{ij}^2\right)^{1/2}$. In the following calculations, V and V_* generally correspond to the total l channels ($i = 1 \ldots l$) except in sections 4.1 and 3.2.4, where they are also used as single-channel signals to obtain the channel-based RE.

Since the transformations shown by equations (8)–(10) from V_a or V_e to V are linear operations, we only need to check the performance according to the potential of a single dipole and noise independently, and the performance according to various dipole combinations or dipole noise combinations can be deduced according to the linearity of the standardization operation. To understand the effectiveness of REST for different dipole locations and orientations, simulations were conducted for each voxel of a discrete cubic grid as a source position with each of the three unit dipoles (Px, Py, Pz) directed along the three Cartesian coordinate (x, y, z) directions separately. The discrete cubic grid consisting of 1269 voxels was created in the brain region confined within radius $r <= 0.86$ (the inner radius of the skull is 0.87, and the dipole layer was located at 0.869, which is between 0.86 and 0.87). The grid started at $(x, y, z) = (0.0, 0.0, 0.0)$ with inter-grid distance of 0.105. The total dipoles tested are 1269 (voxels) $\times$ 3 (dipoles at each voxel) $= 3807$, and for each of the 3807 dipoles we obtained the V, V_a and V_e according to equations (1), (3), (6) and (11). Then we obtained the V' by equations (8) (or (9)) and (10), and an RE(average), an RE(earlobe) and an RE(standardization) pertaining to $V_* = V_a$, $V_* = V_e$ and $V_* = V'$ in equation (12), respectively. In short, for each voxel, we obtained nine REs pertaining to the three dipoles (Px, Py, Pz) and three references (average, earlobe and standardization).

3.2. Simulation results

3.2.1. Comparison between earlobe reference and average reference. In this simulation study, the parameters in equation (11) were $t_0 = 35^* dt$, $f = 10$ Hz, $\gamma = 5$ and $\alpha = \pi/2$ and an earlobe reference was assumed at scalp location $(x, y, z) = (0.049413, 0.964661, 0.258819)$, i.e. the left earlobe. A slice display of the volume distribution of RE(earlobe) is shown in figure 2 (upper row). Apparently, the RE(earlobe) depends not only on the dipole orientation (the differences among the three figure parts in the upper row) and dipole location (the non-constant value in each figure part), but also on the reference site (the RE distribution in each of the three figure parts is clearly around the reference position).

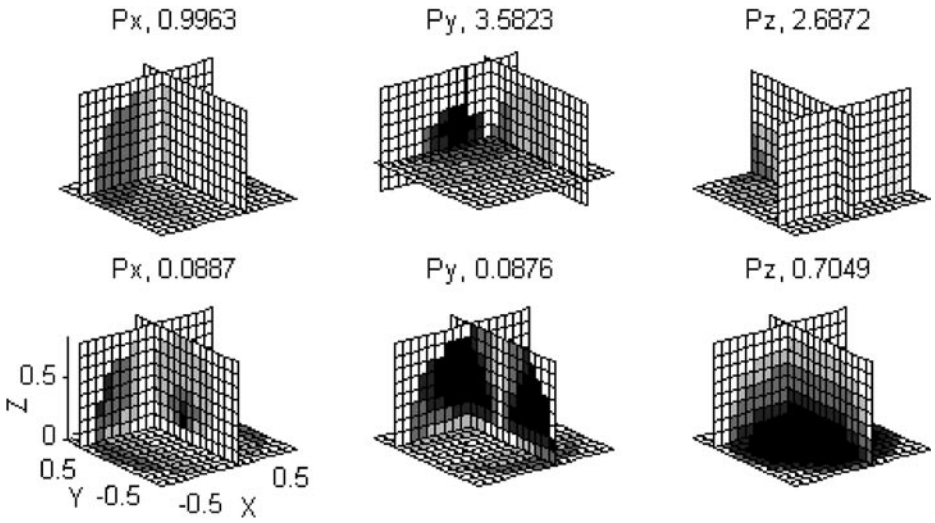

Figure 2. Slice display of the volume distribution of the relative error (RE). The upper row shows RE(earlobe) between the potential with a reference at infinity and the potential with the left earlobe reference. The lower row shows RE(average) between the potential with a reference at infinity and the potential with the average reference. The white points are zero, and the blackest point is the maximum value as shown over each figure part. Px, Py and Pz indicate the dipole sources orientated along the three Cartesian coordinates: x-axis, y-axis and z-axis, respectively.

The reason is that the smaller the distance between the source and the left earlobe, the larger the $\boldsymbol{v}_e$ value (equation (2)) is and the larger the distortion caused by subtracting $\boldsymbol{v}_e$ (equation (3)) is. As a comparison, a slice display of the volume distribution of RE(average) is shown in the lower row of figure 2. Comparing RE(earlobe) with RE(average), we see that the largest RE of RE(earlobe) (358.23% of a Py dipole) is much larger than that of RE(average) (70.49% of a Pz dipole). In addition, for the average reference, RE(average) depends on the virtual average reference, and it does not depend on a specific scalp point. So if the volume conductor and the electrode montage have rotational symmetry, as is the cases in our simulation study, RE(average) also has rotational symmetry as shown by the lower right figure part of figure 2. In fact, we found the largest RE(average) 8.87% of Px dipoles is almost the same as the largest RE(average) 8.76% of Py dipoles, while the largest RE(earlobe) 99.63% of Px dipoles is distinctly different from the largest RE(earlobe) 358.23% of Py dipoles (figure 2 (upper row)), and these differences between the average and the earlobe or a scalp point reference provide the basic reasons that the average reference is more widely used in current EEG/ERP practice.

3.2.2. The RE distribution and effects of electrode number. From the equivalence shown by equations (6) and (7), the standardization result from an earlobe reference was almost the same as that from the average reference, and so, from now on, only the results for the average reference are shown. In addition, as RE(standardization) depends on a virtual point at infinity, not a specific point on the scalp, and both the head model and the electrode montage used here are of rotational symmetry, the volume distribution of RE(standardization) also is approximately rotationally symmetric in theory, and, based on the rotational symmetry, we only need to check RE(average) and RE(standardization) in an upper quarter section of a coordinate plane of the Cartesian coordinate system shown in figure 1, for example, the quarter section of the XOZ coordinate plane with positive x and z. (The approximation of the

rotational symmetry of RE(average) and RE(standardization) is due to the limited number of electrodes. However, the deviation from strict symmetry was small in our simulations, so we assume it to simplify the plots.)

Figures 3(a)–(c) show the RE distribution in the upper quarter section of the *XOZ* coordinate plane with positive x and z. The upper row in each figure part is RE(average), and the lower row is RE(standardization). RE(average) is caused by the deviation of the average of scalp potentials (equation (4)) from zero assumed in the average reference recording model, and this deviation is different for a dipole at different locations with different orientations. The larger the deviation is, the larger the RE is. Figures 3(a)–(c) show that RE(average) of a Pz dipole is always much larger than that of a Px or a Py dipole. The largest RE(average) of Pz dipoles is about 70%, and the smallest RE(average) of Pz dipoles is about 40%. However, the largest REs(average) of Px and Py dipoles are about 8% and about 1%, respectively, and their smallest values are almost zero. The reason is that a spherical cap electrode montage mainly covers either the potential of the positive pole or that of the negative pole of a vertical dipole (Pz), so the average of the potential is usually distinctly different from zero. However, a spherical cap electrode montage generally covers the potentials of both the positive and negative poles of a transverse dipole (Px, Py) especially the tangential dipole (Py) in some positions of the *XOZ* coordinate plane, so the average of the potentials is usually close to zero.

The lower row in each figure part of figures 3 and 4 is the result of REST from potentials with the average reference. The effectiveness of REST is revealed by the difference between the upper row and lower row of each figure part. Based on these figures, we have the following. (1) If the original RE(average) is large such as the RE(average) of a Pz dipole, REST is very effective as shown by the third column of figure 3(a). (2) If the original RE is very small, for example, in the second column of figure 3(a), the largest RE(average) of Py dipoles is only 0.15%, then REST cannot make any further improvement, and it may even enlarge the error to about 1% because of the approximation of the algorithm implementation. (3) The dependence on the source location is different between RE(average) and RE(standardization). For RE(average), the large REs(average) of Px and Py dipoles are in the shallow brain region, while for RE(standardization), the large REs(standardization) of Px and Py dipoles are in the deep brain region. This means REST is specifically efficient for the most important superficial cortex region. (4) The differences among figures 3(a), 3(b) and 3(c) show that a denser electrode array is better for REST to reduce REs(average). Concretely, a dense electrode array is much better than a sparse array in reducing REs(average) of Px and Py dipoles, while the efficiency difference between a dense and a sparse array is not very distinct in reducing RE(average) of a Pz dipole because of the above noted reason that only about half field of the potential distribution of a Pz dipole is recorded by an upper spherical cap electrode array no matter how dense it is. The only way to reduce RE(average) of a Pz dipole is to have a global electrode array; for example, our test showed that if a global 128-electrode array was used, the largest RE(average) of Pz dipoles is also about 1%, which is almost the same as that of Px or Py dipoles. However, a global electrode montage is not feasible in clinical practice.

3.2.3. Effects of volume conductor model. The effects of the volume conductor model were evaluated by assuming that the V_a is calculated by using the above-noted three-concentric-sphere head model, while the reference standardization matrix R_a in equation (8) is formed from a different model. In our tests, we have assessed two cases. One is a modified three-concentric-sphere model with radii 0.87 (brain surface), 0.95 (skull surface) and 1.0 (scalp surface), and conductivities 1.0 (brain and scalp) and 0.2(skull), respectively. Another is an oversimplified model–a single sphere with radius 1.0 and conductivity 1.0. The forward theory of a dipole in a single sphere is given by Yao (2000b). The results are shown in

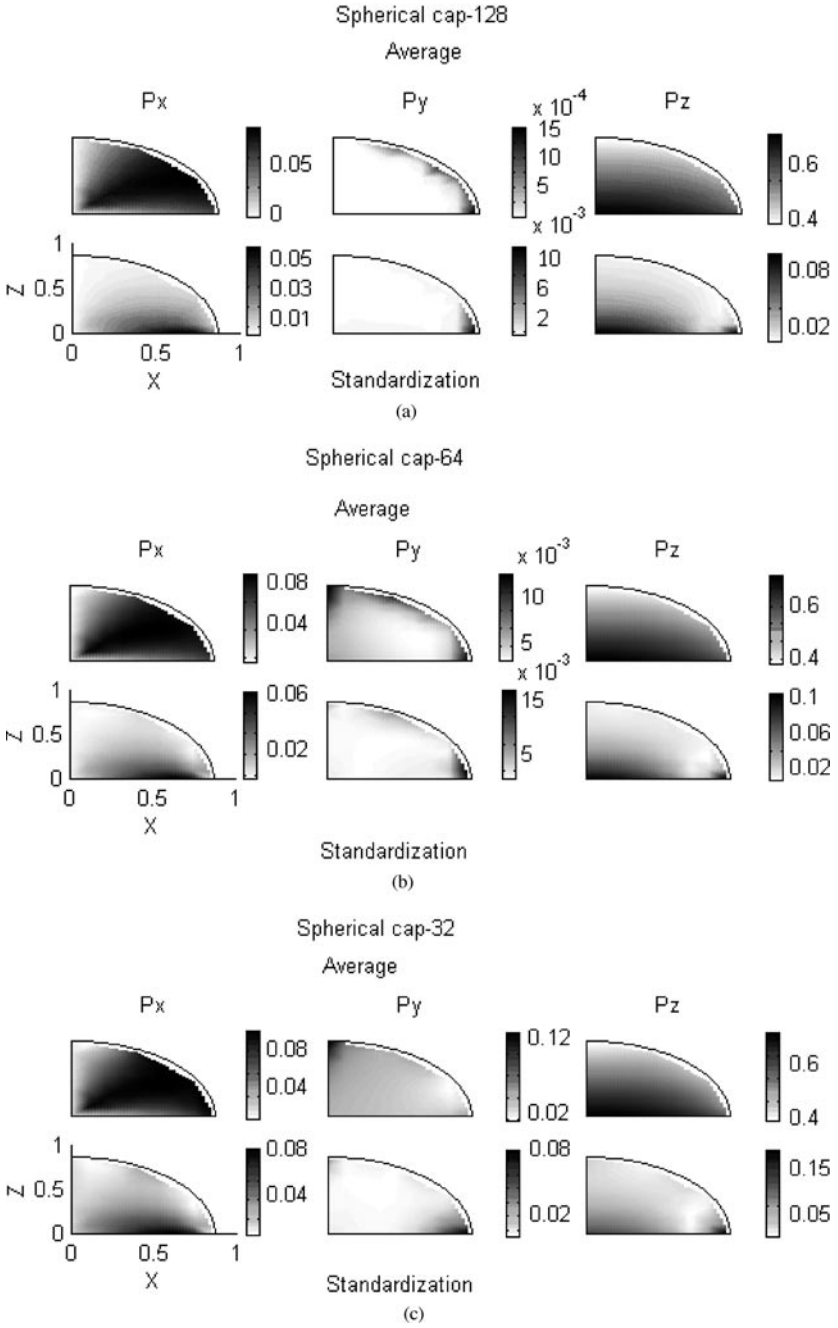

Figure 3. Effects of electrode number. Each map is a section distribution of the REs. RE(average) is shown by the upper row of each figure part and RE(standardization) is shown by the lower row. The section is the *XOZ* plane with positive x and z of the Cartesian coordinate plane. The whitest point corresponds to the smallest value, the blackest point corresponds to the maximum value. The three columns correspond to dipoles with orientations along $x(Px)$, $y(Py)$ and $z(Pz)$ axes respectively. In accordance with the section plane, each Py is a tangential dipole, and the Px, Pz dipoles are the two coordinate components of a radial dipole. The electrodes are uniformly distributed on the upper spherical cap, and the electrode numbers are shown after the 'Spherical cap-' in the figure parts.

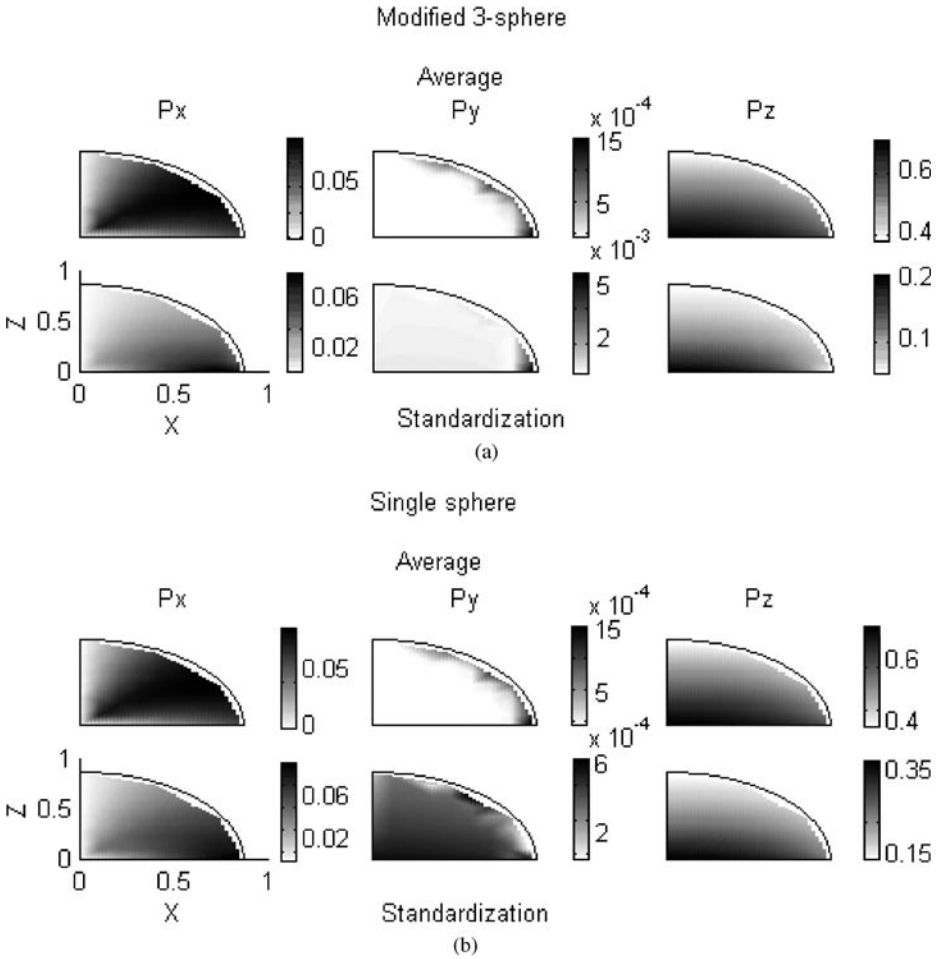

Figure 4. Effects of conductor head model. The electrode number is 128. The meanings of other parameters are the same as those in figure 3. (a) is the situation where the medium parameters of the skull layer in the three-concentric spheres are modified. The radii are modified to 0.87, 0.95 and 1.0, and the conductivities are modified to 1.0 (brain and scalp) and 0.2 (skull). (b) is the situation where the skull layer is replaced by a conductor the same as the brain, and so the model is reduced to a single-sphere model.

figure 4, where the number of electrodes used in the calculation is 128. The basic characteristics are the same as those shown in figure 3, i.e. the RE(average) in shallow region is larger than the RE(standardization); however, the difference, the effectiveness of REST, is not so distinct as that shown by figure 3. For example, the REs(average) of Pz dipoles in the shallow cortex region are about 40%, and the corresponding REs(standardization) are about 15% after standardization using a single-sphere model (figure 4(b)) or about 8% (figure 4(a)) using the modified three-concentric-sphere model, and they are about 2% by using the exact three-concentric-sphere model (figure 3(a)). These results on one hand mean that a detailed head model is preferred to an approximate model for a good reference standardization, and on the other hand they show that the standardization is still beneficial even using an oversimplified head model (single sphere) in reducing the RE because the RE(standardization) of a Pz dipole

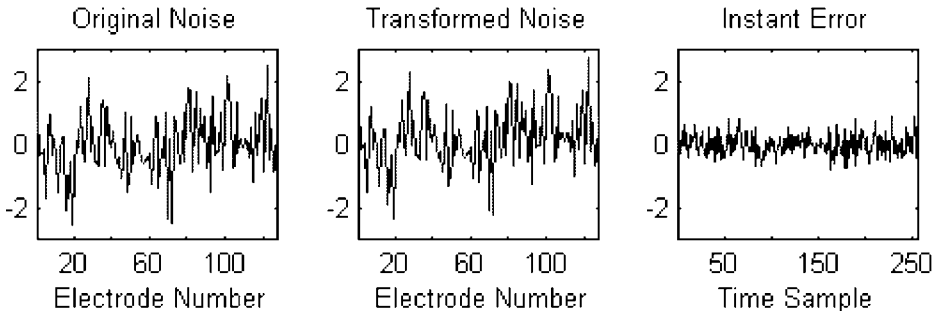

Figure 5. The effect of noise. On the left (original noise) is an instant noise distribution in the 128 electrodes, in the middle (transformed noise) is the output of the original noise undergoing the standardization operation, and their difference is 0.1845 at each electrode position. On the right is the curve of the difference time course of the 256 instant noises used in our study, where the first point is 0.1845.

still was reduced to about half of the RE(average), i.e. from the range 40–70% of REs(average) to 15–35% of REs(standardization), respectively.

3.2.4. Effect of noise. Due to the linearity of equations (8) and (9), and in order to understand the noise effect independently, a test using only noise as the input to the standardization operator R_a was carried out in this work. Here the noise is a Gaussian white noise generated by Matlab, and it is used to mimic the noise of the environment and instrument noise. According to equations (8) and (10), we obtain $N' = N + \boldsymbol{t}\,\text{average}(N')$. The standard deviation and mean value of the original input noise (corresponding to the 128 (channels) $\times$ 256 (samples) $=$ 32768 points) is 0.993382 and 0.00, while the counterparts of the output N' are 1.044484 and 0.006930. The ratio between 1.044484 and 0.993382 is 1.051 and the difference between the averages is 0.006930. These facts mean that the noise content in total is kept almost the same in the transformation. However, the difference between N and N', the average(N'), is different from one moment to another, and the RE is 32.4% calculated by equation (12) with $V = N$ and $V_* = N'$ for the whole 32768 points. If the RE is calculated channel by channel, then the maximum channel-based RE is 35.73% at channel 48 and the minimum is 29.25% at channel 37 in this example. In figure 5, N(original noise) and N'(transformed noise) are illustrated on the left and in the middle by their values in 128 channels at an instant, the difference, i.e. average(N') at this instant, between them is 0.1845 at each channel position. However, the value average(N') is different from one instant to another as shown on the right of figure 5 (256 latency points), which looks like a random series with standard deviation and mean value being 0.3338 and –0.0021, respectively. This fact means that when noise exists in the data, the standardization may introduce an instant constant value to each channel, and such a value may be a positive or a negative number which depends on the instant noise distribution on the scalp.

In an ideal case, if the average(N) were zero, the standardization should not introduce a non-zero average(N'). However, REST is based on the prior assumption that the sources of the recordings are inside the equivalent dipole layer, and the net noise recordings are not able to be considered as potentials generated by sources inside the closed equivalent layer, so they cannot be standardized to a point at infinity by REST. In this test, the net noise recordings are used as V_a in equation (8), so it is assumed to be the potentials produced by sources inside the closed equivalent layer, and the standardization accordingly recover an 'average(N')' whose value is determined by the instant noise distribution on the scalp surface. As the noise distribution

on the scalp generally changes randomly from one instant to another, the wrongly recovered 'average(N')' also changes randomly from one instant to another as shown by the right figure part in figure 5.

4. Simulation study (II): significance of REST in temporal analysis

4.1. Dynamic effect of the average artefact

As a scalp point reference or the average reference for EEG varies with each latency (Desmedt *et al* 1990), the temporal and frequency analysis are related to the reference. In this section, the dynamic effect of the average artefact and the effectiveness of REST in removing the average artefact are shown by the differences of the time courses and spectra of simulated EEG recordings with a reference at infinity, the average reference and the recovered EEG recordings with a reference at infinity.

Suppose there are three dipoles in the volume conductor. The locations of the three dipoles are respectively at $(-0.42, -0.21, 0.525)$ $(r = 0.7044)$, $(-0.21, 0.42, 0.630)$ $(r = 0.7857)$ and $(-0.315, -0.105, 0.735)$ $(r = 0.8065)$. They all are radial dipoles. The strength of the first two is one unit, and that of the third one is half a unit. The temporal process is defined by equation (11) with the parameters $t_0 = 35^* dt$, $f = 10$ Hz, $\gamma = 5$, $\alpha = \pi/2$ for dipole 1, $t_0 = 40^* dt$, $f = 11$ Hz, $\gamma = 4$, $\alpha = \pi/2$ for dipole 2 and $t_0 = 80^* dt$, $f = 8$ Hz, $\gamma = 6$, $\alpha = 0$ for dipole 3.

Figure 6(a) shows recordings at nine electrodes. Their order numbers in the 128 electrodes are shown, which are selected from channel 1 with an interval of 16 except channel 41, the channel with the maximum difference before and after the standardization in the 128 channels. For this example, the global RE(average) is 35.5%, and after standardization, the global RE(standardization) is only 0.6%. If we check each channel with formula (12), we obtain the channel-based RE distribution. As shown in figure 6(b), the maximum channel-based RE(average) and RE(standardization) are at channel 41, which is the channel with the smallest signal energy, and the minimum channel-based RE(average) and RE(standardization) are at channel 15, which is the channel with the largest signal energy. The reason is that the numerator in the formula of the channel-based RE calculation is the reference error and the incomplete standardization error, which are the same for all channels; the only difference is the denominator, which is the channel signal energy in the formula of the channel-based RE calculation, so the larger the signal energy is, the smaller the RE is. Viewed from figure 6(a), the waveforms of recordings with average reference are distinctly different from those with reference at infinity, and the waveforms of the standardized recordings are almost the same as those with reference at infinity. Checked from figure 6(b), the channel-based RE is reduced from 13.91 (minimum)–690.61% (maximum) to 0.24 (minimum)–11.76% (maximum), respectively. Apparently, REST attains great success and it is due to this that the adopted sources here all are located in the effective shallow source region of REST as illustrated in figures 2 and 3.

Figure 7 shows the normalized strength of the Fourier spectra of the nine channels, where the difference between the desired potential referenced at infinity and the practical potential referenced at average is quite distinct. And such a great difference between the spectra of average reference data (before standardization) and that of the desired data referenced at infinity may result in a misleading in the explanation of the temporal dynamic process such as EEG rhythm analysis. Figure 7 shows that the actual spectra are nicely reconstructed, and such a result means that the spectral analysis of EEG can be possibly made more objective and realistic by the application of REST.

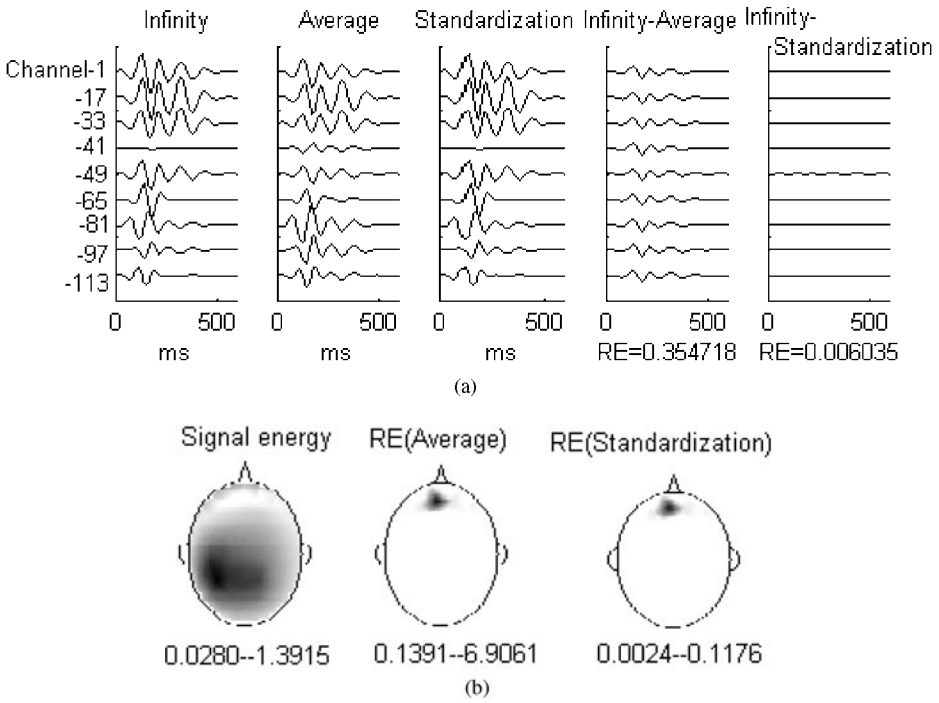

Figure 6. Simulated scalp recordings and standardization result. (a) Time course analysis. The horizontal axis is in milliseconds. The channel order number is shown on the left of the first column. From left to right, the first is the recording with reference at infinity, followed by the average reference, and then the reference at infinity (*standardization*). The last two are the two differences *infinity* − *average* and *infinity* − *standardization*. The global RE between *infinity* and *standardization* is 0.6035%, and that between *infinity* and *average* is 35.4718%. (b) Signal energy and channel-based relative error distribution. The values shown below each figure part are the maximum (the blackest point) and the minimum value (the whitest point in the figure). From left to right, the first is the L2 norm signal energy distribution over the scalp surface; the maximum value 1.3915 locates at channel 15 with Cartesian coordinates (−0.355361, 0.494277, 0.793353); the minimum 0.0280 locates at channel 41 with Cartesian coordinates (0.762777, 0.070682, 0.642788). The second is the distribution of the relative errors of the average reference calculated channel by channel; the maximum is 690.61% at channel 41, and the minimum is 13.91% at channel 15, followed by the distribution of the relative errors after standardization, the maximum is 11.76% at channel 41, and the minimum is 0.24% at channel 15.

4.2. An empirical example

Figures 8 and 9 show results of an empirical example. The number of electrodes is 120, with their positions defined as the projection points on the corresponding best-fit sphere surface of group-averaged electrode positions over ten subjects (NeuroScan, Inc, USA). Then the sphere surface is normalized to the three-concentric-sphere head model. The potential data are a group-averaged VEP over ten subjects. Due to an obvious artefact in channel 86, only the remaining 119 channels are used in the calculation. The visual stimulation is a checkerboard flashed to the right visual field. The recordings are from –200 to 1200 ms time locked to the stimulation. Here, as the number, 119, and positions of electrodes are different from the above simulations, the *Ra* was reconstructed according to the practical 119-electrode montage with the three-concentric-sphere head model and the equivalent dipoles layer model used in

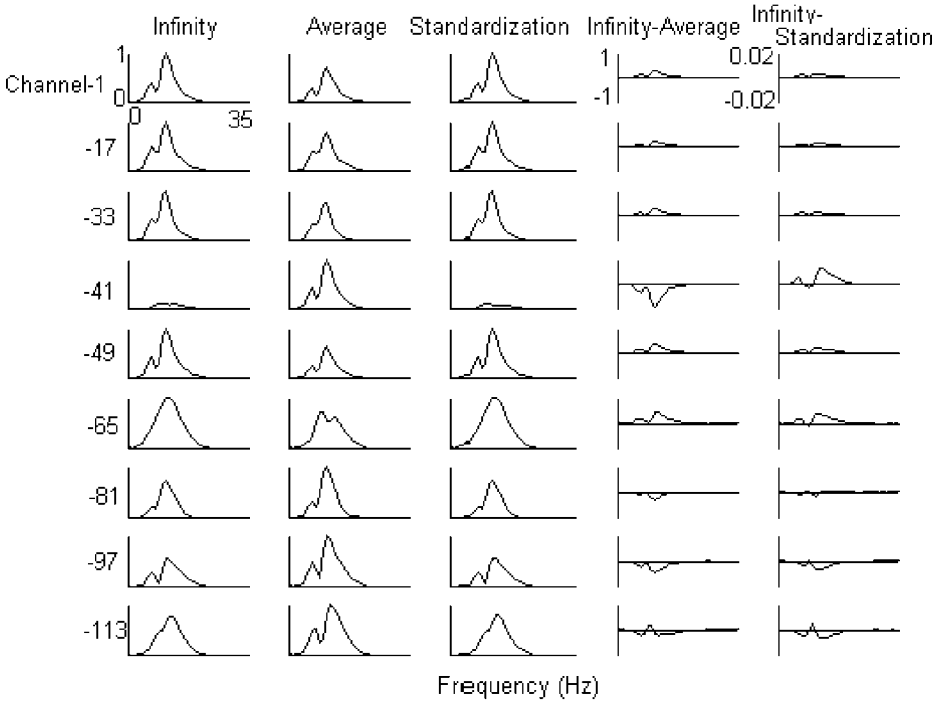

Figure 7. Normalized strength of the Fourier spectra of the nine scalp recordings shown in figure 6. The displaying range of the frequency axis is from 0 to 35 Hz. The values of the five curves are normalized by the maximum value of the *infinity*, *average* and *standardization* of each channel. The first three columns are displayed in the range [0 1] for they are always positive. The fourth column is displayed in the range $[-1\ 1]$. The fifth column is displayed in the range $[-0.02$ 0.02] for its values are small.

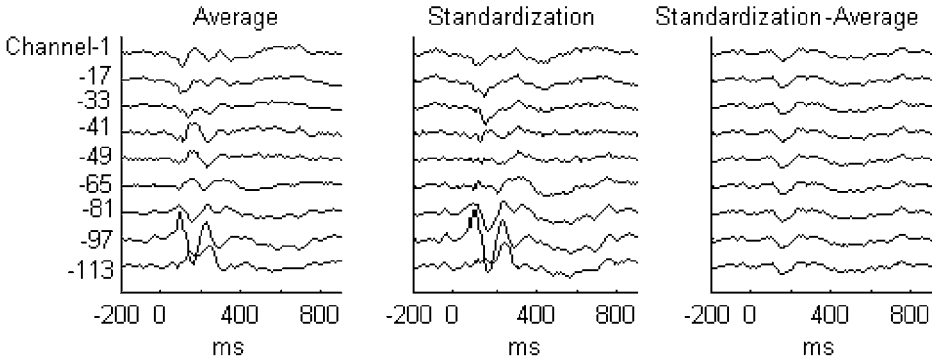

Figure 8. Empirical recordings test. The horizontal axis is in milliseconds. The *average* is the practical recordings, the *standardization* is the result of the reference standardization. (The data were provided by the Beijing Laboratory of Cognitive Science, University of Science and Technology of China.)

figure 3(a). After we obtained the *Ra*, the remaining calculations were the same as those in simulations.

Figure 8 shows nine of the 119 channels. The *average* is the empirical recordings, the *standardization* is the result after standardization, and the *standardization* − *average* is the

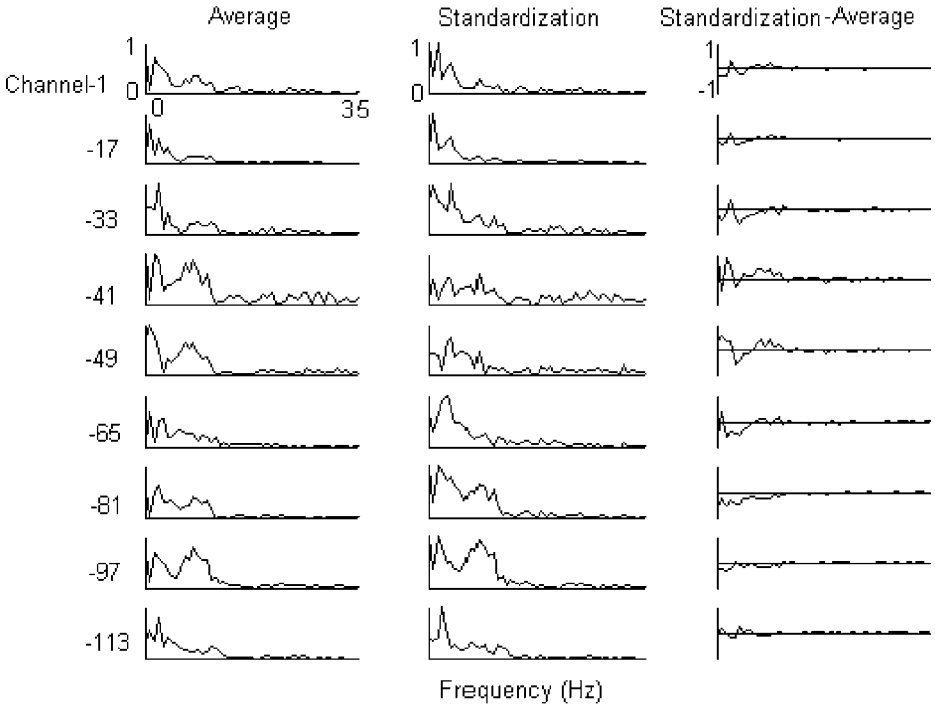

Figure 9. Normalized spectrum display of the nine scalp recordings shown in figure 8. The display range of the frequency axis is from 0 to 35 Hz. The values of the three curves are normalized by the maximum value of the *average* and *standardization* of each channel. The first two columns are displayed in the range [0 1] for they are always positive. The third column is displayed in the range [−1 1].

restored component. The RE calculated by equation (12) with $V = \textit{standardization}$ and $V_* = \textit{average}$ is 58.31%, and the maximum channel-based RE is 135.63% occurring at channel 59 with Cartesian coordinates $(x, y, z) = (0.326, -0.861, 0.390)$.

Figure 9 shows the spectra of the nine channels before and after standardization. Both figures 8 and 9 show that some large values are introduced into some channels by REST. Viewing figure 8, the modification occurs not only in 'potential values' but also in polarity and latencies of peaks, and as such parameters are used in explanation of VEP data the standardization is of significance for VEP application.

5. Discussion and conclusion

5.1. Summary of the work reported above

The work reported above is based on two facts. (1) The choice of a particular reference does not in any way change the theoretical relation between sources and scalp potentials (Geselowitz 1998). (2) As the real sources inside the brain and their equivalent sources produce the same scalp potentials, the potentials with a reference at infinity may be approximately recovered from the equivalent sources reconstructed approximately by EST from the potentials with the average reference, where the reconstruction approximation of the equivalent sources is due to the imperfect information of the head model and limited scalp measurements, and the degree of approximation is different for different source location and orientation as shown by the

simulations. However, our simulation results show the RE could be reduced for some source locations especially the most important upper shallow cortex region of the brain. The main shortcoming of REST is the limited ability to reduce the RE of deep sources. In practice, if you find some changes such as the polarity and latencies of peaks after using REST, and you do not know whether the sources are in a deep or shallow region, then it is difficult to judge the correctness of the changes of the peaks.

5.2. REST and other reference-free techniques

After going through the above sections, the relations between REST and other reference-free techniques should be considered, for example the LMT (Hjorth 1975), where the effects of the bias imposed by using a physical reference is neutralized by computing differential measures of the data (Gencer *et al* 1996). However, this methodology emphasizes shallow and localized sources because the differential calculation acts as a spatial high-pass filter, and the high-spatial-frequency components on the scalp surface of shallow and localized sources are more abundant than those of deep or smooth distributed sources. In fact, the Laplacian is different from electric potential in physics; it is approximately proportional to the flux of the entrant current flowing from the scalp into the skull. And so a reference-free potential or a reference-effect reduced potential like that given by REST in practice is important for itself no matter whether the Laplacian can or cannot be precisely deduced from the potential or be directly measured. Moreover, the current state of Laplacian estimation from the potential is definitely far from a precise reconstruction of the actual Laplacian (Nunez *et al* 1994, Yao 2000a), and the direct measurement of the *Laplacian* is still a problem without a determined conclusion (Geselowitz and Ferrara 1999).

Another reference-free technique is the magneto-encephalogram (MEG). Both EEG and MEG are due to the neural electric current sources; however, they are different in the response of the sources in practice. The MEG collected by a coil detector with its axis normal to the scalp surface is usually a recording of the vertical component of the whole magnetic flux vector. Alternatively, say the MEG does not see a radial source, but only a tangential source, while the EEG sees both the radial source and tangential source, and so a combination of EEG and MEG is encouraged in solving the inverse problem (Cohen and Cuffin 1987).

The presented REST is a new application of EST, and the difference between REST and CIT is the method of application of EST. The cortical potential reconstructed by EST may be referenced at a scalp point or at a point at infinity; when it is referenced at infinity, it may be considered as a reference-free cortical potential; however, such a property has never been emphasized in the literature to my knowledge. The reason is that the cortical imaging technique mainly focuses on improving the spatial resolution by extrapolating the scalp potential inward to the cortical surface, and in this extrapolation process, there is an amplification of the high spatial frequency components because the factor $[1/r^{l+1}(r = 0.87,$ *cortical surface*$)]/[1/r^{l+1}(r = 1.0,$ *scalp surface*$)]$ is larger for a larger l than that for a smaller l, and the larger l corresponds to the higher spatial frequency component (Yao 2000a). Apparently, as noise existing in scalp EEG recordings is generally of wide spectrum, its amplification is larger than the real EEG signal, so such an inward extrapolation is an unstable process (Dampney 1969). In order to stabilize this extrapolation process, a noise smooth technique such as various regularization techniques has to be involved (Sidman *et al* 1992, Babiloni *et al* 1997, Yao 2000a). In general, the regularization is used with apparent subjective interference for a good spatial mapping (Sidman *et al* 1992). The final reconstructed cortical potential with apparent enhanced spatial resolution compared to the scalp potential then is definitely different from the actual cortical potential, so the 'reference-free' property in

the temporal aspect is definitely changed by such an objective process. In REST, only the reference is transformed to a point at infinity, no inward extrapolation is involved and so the noise may be changed but the amount of noise is maintained almost unchanged as shown by the noise test. We can therefore keep the algorithm in a primary form without involving any subjective regularization and weight processing. In other words, though the current REST and the CIT originally described by Sidman *et al* are based on the same EST, their focuses are different. REST focuses on the temporal information restoration on the scalp by recovering the zero-spatial-frequency information (a constant for all electrodes), where no inward extrapolation is involved and so no subjective regularization is involved. CIT focuses on a spatial-resolution-enhanced cortical surface mapping by relatively enlarging the high-spatial-frequency components through an inward extrapolation and there a subjective regularization is involved to reduce the wide-spectrum noise amplification caused by such an inward extrapolation. In fact, LMT also mainly focuses on the spatial aspect, and a noise smooth is generally involved because the high-pass spatial filter also amplifies the wide-spectrum noise (Yao 2000a).

5.3. Final comments

As a primary attempt to restore the lost potential of the reference electrode in EEG recordings, the technique is far from complete. For example, the current work is based on the three-concentric-sphere model, and the validity on a realistic head model needs to be evaluated in the future. Besides, in order to convince the validity of the algorithm in empirical data, some phantom experiments are necessary. However, the presented simulations do give us great encouragement, and we believe a final practical algorithm is likely to bring an impact on EEG study. For example, it may raise problems such as whether the spectrum characteristics of various brain states are the same as we obtained through the body reference recordings before. It may also strengthen the application of the multi-channel EEG system to obtain a better EEG temporal analysis by REST.

Many researchers in the field of electrophysiology yearn for the discovery of a reference-free potential measurement. In fact, a reference-free or reference-independent potential cannot be measured. Our contribution here is just to show that the effect of the reference could be reduced and so an improvement of the temporal analysis including the spectral analysis could be made.

Acknowledgments

This work is supported by the NSFC (No 39980009), the Foundation for University Key Teacher by the MOE of the People's Republic of China and the excellent Young Teachers Programme of MOE, PRC. The author wishes to thank the unknown referees for their constructive comments. The author would also like to thank Professor L Chen and S Fan and Zhou Y and Zeng M for discussions.

References

Babiloni F, Babiloni C, Carducci F, Fattorini L, Anello C, Onorati P and Urbano A 1997 High resolution EEG: a new model-dependent spatial de-blurring method using a realistically-shaped MR-constructed subject's head model *Electroenceph. Clin. Neurophysiol.* **102** 69–80

Cohen D and Cuffin B N 1987 A method for combining MEG and EEG to determine the sources *Phys. Med. Biol.* **32** 85–9

Dampney C N G 1969 The equivalent source technique *Geophysics* **34** 539–53

De Munck J C 1988 The potential distribution in a layered anisotropic spheroidal volume conductor *J. Appl. Phys.* **64** 461–70

Desmedt J E, Chalklin V and Tomberg C 1990 Emulation of somatosensory evoked potential (SEP) components with the 3-shell head model and the problem of 'ghost potential fields' when using an average reference in brain mapping *Electroenceph. Clin. Neurophysiol.* **77** 243–58

Gencer N G, Williamson S J, Gueziec R and Hummel R 1996 Optimal reference electrode selection for electric source imaging *Electroenceph. Clin. Neurophysiol.* **99** 163–73

Geselowitz D B 1998 The zero of potential *IEEE Eng. Med. Biol.* No 1 128–32

Geselowitz D B and Ferrara J E 1999 Is accurate recording of the ECG surface Laplacian feasible? *IEEE Trans. Biomed. Eng.* **46** 377–81

He B, Wang Y, Pak S and Ling Y 1996 Cortical source imaging from scalp electroencephalograms *Med. Biol. Eng. Comput.* **34** (suppl. 1) 257–8

Hjorth B 1975 An online transformation of EEG scalp potentials into orthogonal source derivations *Electroenceph. Clin. Neurophysiol.* **39** 526–30

Jackson J D 1975 *Classical Electrodynamics* (New York: Wiley) pp 40–5

Niedermeyer E and Lopes da Silva F 1999 *Electroencephalography Basic Principles, Clinical Applications and Related Fields* 4th edn (Baltimore, MD: Williams and Wilkins)

Nunez P L, Silberstein R B, Cadusch P J, Wijesinghe R S, Westdrop A F and Srinivasan R 1994 A theoretical and experimental study of high resolution EEG based on surface Laplacians and cortical imaging *Electroenceph. Clin. Neurophysiol.* **90** 40–57

Pascual-Marqui R D and Lehmann D 1993 Topographical maps, sources localization inference, and the reference electrode: comments on a paper by Desmedt *et al Electroenceph. Clin. Neurophysiol.* **88** 532–3

Rush S and Driscoll D A 1969 EEG electrode sensitivity—an application of reciprocity. *IEEE Trans. Biomed. Eng.* **16** 15–22

Sidman R, Vincent D, Smith D and Lee L 1992 Experimental tests of the cortical imaging technique—applications to the response to median nerve stimulation and the localization of epileptiform discharges *IEEE Trans. Biomed. Eng.* **39** 437–44

Wang Y and He B 1998 A computer simulation study of cortical imaging from scalp potentials *IEEE Trans. Biomed. Eng.* **45** 724–35

Wolpaw J R and Wood C C 1982 Scalp distribution of human auditory evoked potentials. I. Evaluation of reference electrode sites *Electroenceph. Clin. Neurophysiol.* **54** 15–24

Yao D 1995a Equivalent source method and three-dimensional EEG imaging *J. Biomed. Eng.* **12** 322–41 (in Chinese)

——1995b Study of complex Huygens' principle *Int. J. Infrared Millimeter Waves* **16** 831–8

——1996 The equivalent source technique and cortical imaging *Electroenceph. Clin. Neurophysiol.* **98** 478–83

——2000a High-resolution EEG mappings: a spherical harmonic spectra theory and simulation results *Clin. Neurophysiol.* **111** 81–92

——2000b Electric potential produced by a dipole in a homogeneous conducting sphere *IEEE Trans. Biomed. Eng.* **47** 964–6

Yao D and Luo B 1996 Theory of the EEG cortical imaging techniques *Chin. J. Biomed. Eng. (Engl. Edn)* **5** 128–36

Yao D, Zhou Y, Zeng M, Fan S, Lian J, Wu D, Ao X, Chen L and He B 2001 A study of equivalent source techniques of high-resolution EEG imaging *Phys. Med. Biol.* **46** 2255–66